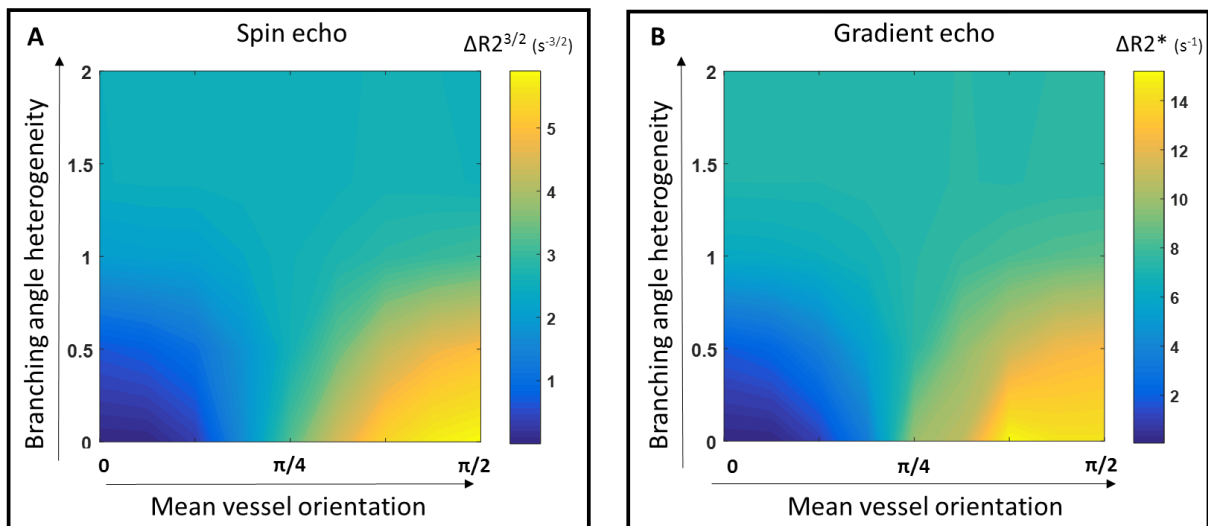


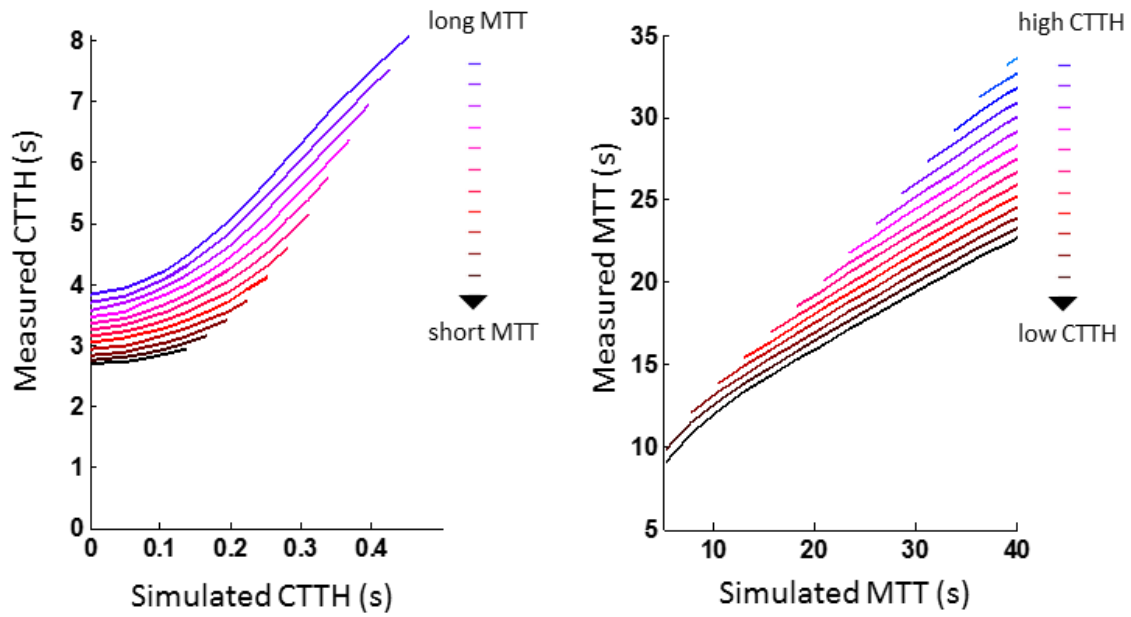
Supplementary

	Patient 1	Patient 2	Patient 3	Patient 4	Patient 5
Gender	Male	Male	Male	Male	Male
Age	76	66	69	57	63
Diagnosis	Glioblastoma (WHO gr IV)	Glioblastoma (WHO gr IV)	Glioblastoma (WHO gr IV)	Glioblastoma (WHO gr IV)	Glioblastoma (WHO gr IV)

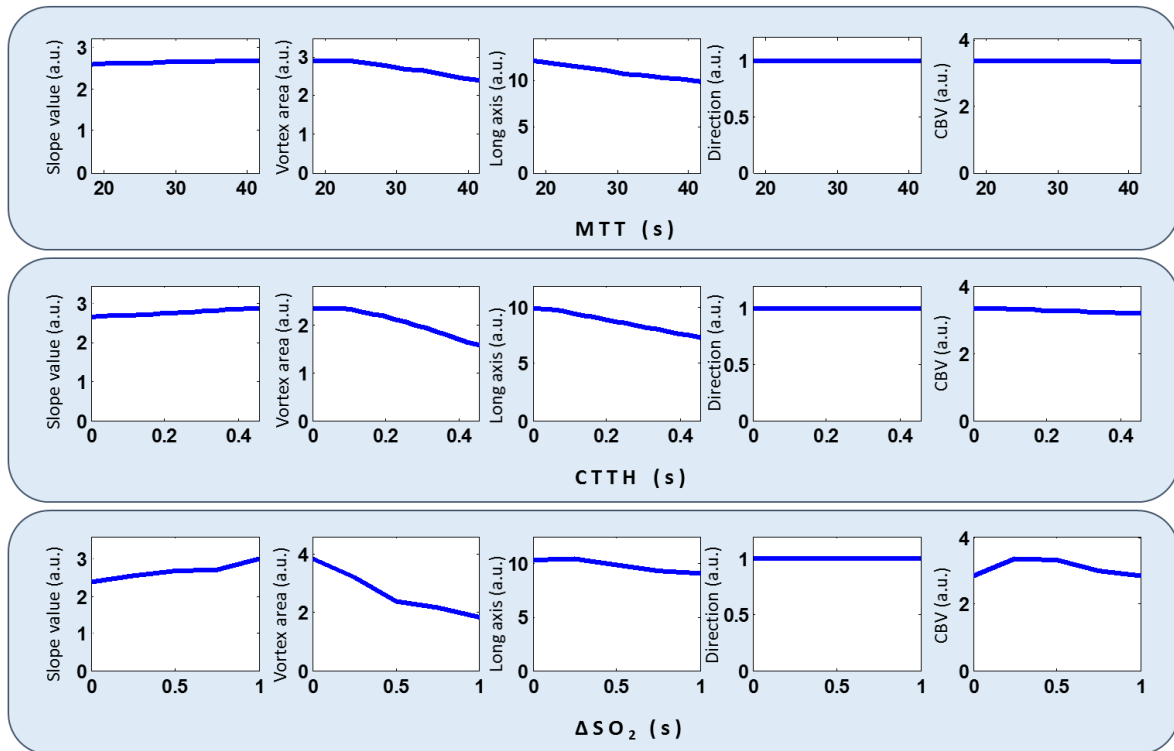
Supplementary Table 1. Gender, age and diagnosis of patients. Patient constitutes a homogenous group, as patients are all males, age from 57-76 years with glioblastoma.



Supplementary Figure 1: The effects of vessel orientation distributions on the relaxation rates from gray matter-like branching structured vessel trees. The relaxation rates from spin echo [A] and gradient echo [B] are independent of mean vessel orientation when branching angle heterogeneity is high ($\sigma > 1$). With lower branching angle heterogeneity ($\sigma < 1$), the relaxation rates increase when mean vessel orientation approaches $\pi/2$, in accordance with what was found for white matter-like vessel trees.



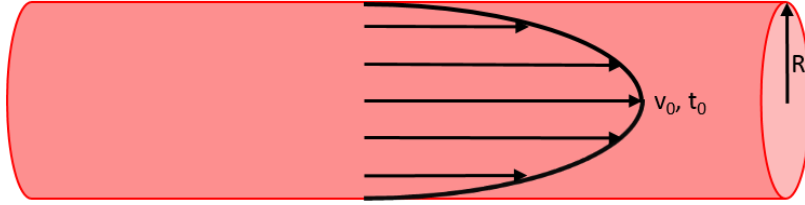
Supplementary Figure 2: **[A]:** Estimated values of CTTH (y-axis) scales with the true CTTH of the simulated vessel system (x-axis), but increases as the MTT increases (black to blue lines). The measured CTTH never approaches zero, even when the simulated CTTH is set to zero. This is due to the implementation of transit time distribution in the simulation model. In our model, each vessel has a distribution of transit times (equation (4)), resulting in a distribution of transit times at the voxel-level, even for a homogenous distribution of average transit times at the capillary level. This also explains the relative small change in measured CTTH for low values of simulated CTTH – in our model, a substantial increase in simulated CTTH is needed to produce detectable changes in CTTH at the voxel-level. **[B]:** Measured MTT (y-axis) is proportional to the simulated MTT (x-axis), but increases as the CTTH increases (black to blue coloured lines). There is also a slight discrepancy between the numerical values of the measured versus simulated MTT. The definition of $MTT (= \alpha\beta)$ and $CTTH (= \sqrt{\alpha\beta})$ results in the interdependency of MTT and CTTH. Higher CTTH-values results in higher MTT-values and vice versa.



Supplementary Figure 3: VAI-response for varying MTT, CTTH and ΔSO_2 . For increasing MTT (top row), vortex area and long-axis decreases, whereas slope values, direction and CBV-values are unaffected. For increasing CTTH (centre row), vortex area and long-axis decreases, there is a minor increase in slope values, whereas direction and CBV-values are unaffected. For increasing ΔSO_2 (bottom row), vortex area decreases, minor changes can be seen in slope values, long axis and CBV-values, while direction is unaffected.

Supplementary Methods

In our model of the vasculature, the vessels are approximated as cylindrical pipes with laminar flow, as illustrated in Supplementary Figure 3. The largest velocity, v_0 , and the shortest transit time, t_0 , occur at the centre of the cylinder.



Supplementary Figure 3: Vessel approximated as cylinder with laminar flow.

When the geometry of the vessels is known and we assume laminar flow, the velocity profile of a cylindrical pipe is given by

$$v(r) = v_0 \left(1 - \frac{r^2}{R^2}\right) \quad (1)$$

When q is the flow in a concentric cylinder with radius r and Q is the total flow in the cylinder, the fractional flow q/Q is:

$$\frac{q}{Q} = \int_0^r v(r') 2\pi r' dr' / \int_0^R v(r') 2\pi r' dr' = 2 \frac{r^2}{R^2} - \frac{r^4}{R^4} = 1 - \frac{t_0^2}{t^2} \quad (2)$$

The fraction of the flow from t_0 to a later time t is the fraction of the flow which arrives before time t , in other words the cumulative distribution function of transit times $H(t)$:

$$H(t) = \int_{t_0}^t h(\tau) d\tau = \frac{q}{Q} \quad (3)$$

The transport function of the vessel is thus given by:

$$h(t) = \frac{dH(t)}{dt} = \begin{cases} 0, & t < t_0 \\ \frac{2t_0^2}{t^3}, & t \geq t_0 \end{cases} \quad (4)$$